

1 **Targeting Integrated Stress Response by ISRIB combined with imatinib attenuates**  
2 **STAT5 signaling and eradicates therapy-resistant Chronic Myeloid Leukemia cells.**

3  
4 Wioleta Dudka<sup>1</sup>, Grażyna Hoser<sup>2</sup>, Shamba S. Mondal<sup>3</sup>, Laura Turos-Korgul<sup>1</sup>, Julian Swatler<sup>1</sup>, Monika Kusio-  
5 Kobiałka<sup>1</sup>, Magdalena Wołczyk<sup>1</sup>, Agata Klejman<sup>4</sup>, Marta Brewińska-Olchowik<sup>1</sup>, Agata Kominek<sup>1</sup>, Milena Wiech<sup>1</sup>,  
6 Marcin M Machnicki<sup>5</sup>, Ilona Seferyńska<sup>6</sup>, Tomasz Stokłosa<sup>5</sup>, Katarzyna Piwocka<sup>1, #</sup>.

7  
8 <sup>1</sup> Laboratory of Cytometry, Nencki Institute of Experimental Biology, Polish Academy of Sciences, Warsaw,  
9 Poland

10 <sup>2</sup> Center of Postgraduate Medical Education, Laboratory of Flow Cytometry, Warsaw, Poland

11 <sup>3</sup> Laboratory of Bioinformatics, Nencki Institute of Experimental Biology, Polish Academy of Sciences, Warsaw,  
12 Poland

13 <sup>4</sup> Laboratory of Animal Models, Nencki Institute of Experimental Biology, Polish Academy of Sciences, Warsaw,  
14 Poland

15 <sup>5</sup> Department of Tumor Biology and Genetics, Medical University of Warsaw, Warsaw, Poland

16 <sup>6</sup> Department of Hematology, Institute of Hematology and Blood Transfusion, Warsaw, Poland

17 # corresponding author: Katarzyna Piwocka, Nencki Institute, Polish Academy of Sciences, 3 Pasteur Str, 02-093  
18 Warsaw, Poland; +48225842162; e-mail: [k.piwocka@nencki.edu.pl](mailto:k.piwocka@nencki.edu.pl)

19  
20  
21 ISR, ISRIB, GSK2656157, Imatinib, CML, Chronic Myeloid Leukemia, therapy resistance, STAT5, PTPN11,  
22 Patient-Derived Xenograft

23  
24  
25  
26 **Competing Interests statement**

27 The authors declare no competing financial interests.

28  
29 The research was funded by National Science Centre grants: PRELUDIUM (2015/19/N/NZ3/02267) to WD,  
30 Sonata Bis (2013/10/E/NZ3/00673) to KP and HARMONIA (2014/14/M/NZ5/00441) to TS. KP was also supported  
31 by TEAM-TECH Core Facility Plus (POIR.04.04.00-00-23C2/17-00) grant from Foundation for Polish Science co-  
32 financed by the European Union under the European Regional Development Fund.

33

34 **Abstract**

35 Integrated Stress Response (ISR) facilitates cellular adaptation to variable environmental conditions by  
36 reprogramming cellular response. Activation of ISR was reported in neurological disorders and solid tumours, but  
37 its function in hematological malignancies remains largely unknown. Previously we showed that ISR is activated  
38 in chronic myeloid leukemia (CML) CD34+ cells, and its activity correlates with disease progression and imatinib  
39 resistance. Here we demonstrate that inhibition of ISR by small molecule ISRib, but not by PERK inhibitor  
40 GSK2656157, restores sensitivity to imatinib and eliminates CM Blast Crisis (BC) D34+ resistant cells. We found  
41 that in Patient Derived Xenograft (PDX) mouse model bearing CD34+ imatinib/dasatinib-resistant CML blasts with  
42 *PTPN11* gain-of-function mutation, combination of imatinib and ISRib decreases leukemia engraftment.  
43 Furthermore, genes related to SGK3, RAS/RAF/MAPK, JAK2 and IFN $\gamma$  pathways were downregulated upon  
44 combined treatment. Remarkably, we confirmed that ISRib and imatinib combination decreases STAT5  
45 phosphorylation and inhibits expression of STAT5-target genes responsible for proliferation, viability and stress  
46 response. Thus, our data point to a substantial effect of imatinib and ISRib combination, that results in  
47 transcriptomic deregulation and eradication of imatinib-resistant cells. Our findings suggest such drug  
48 combination might improve therapeutic outcome of TKI-resistant leukemia patients exhibiting constitutive STAT5  
49 activation.

50

51

52

53

54

55

56

57

58

59

60

61

62

63

64

65

66

67

68 **Introduction**

69 Chronic myeloid leukemia (CML) which is driven by oncogenic BCR-ABL1 tyrosine kinase, is an example of a  
70 disease that is successfully treated with molecular targeted therapy. Introduction of imatinib significantly improved  
71 CML treatment, patients' life expectancy and overall survival <sup>1,2</sup>. However, although imatinib shows remarkable  
72 clinical efficacy in the chronic phase, the effects in advanced phases are short-lived, complete remissions are  
73 rare, and relapse occurs often <sup>3-5</sup>. Many patients show primary or secondary resistance to imatinib or second  
74 generation tyrosine kinase inhibitors (TKIs), such as dasatinib, nilotinib or bosutinib. The resistance originates in  
75 majority from cellular intrinsic mechanisms. Apart from *BCR-ABL1* point mutations (e.g. T315I) which affect drug  
76 binding affinity <sup>6,7</sup>, the *BCR-ABL1* gene amplification or clonal evolution may lead to relapse driven by both BCR-  
77 ABL1-dependent and -independent mechanisms.

78 The most recognized pathways responsible for resistance are mediated by activation of JAK2/STAT5,  
79 RAS/RAF/MAPK or PI3K/Akt/mTOR <sup>3,8,9</sup>. They activate proliferation, anti-apoptotic response and survival,  
80 cytokine and growth factors signaling, altogether strongly promoting resistance to treatment and disease relapse.  
81 Therefore, targeting these pathways is one of the current strategies for eradication of resistant cells <sup>10-12</sup>.

82 Previously, we identified that the PERK-eIF2 $\alpha$  pathway related to Integrated Stress Response (ISR) is activated in  
83 CD34+ CML-BP cells <sup>13</sup>. ISR is a highly conserved signaling responsible for cell adaptation and survival upon  
84 stress conditions <sup>14-17</sup>. This is achieved by phosphorylation of the eukaryotic translation initiation factor eIF2 $\alpha$ ,  
85 remodelling of translation <sup>18</sup> and transcription of stress response effector genes, including CHOP and GADD34,  
86 which are ISR markers.

87 Under physiological conditions, the ISR is one of the mechanisms sustaining homeostatic balance in a healthy  
88 cell. Cancer cells can utilize ISR to survive and develop drug resistance. Previous reports demonstrated that ISR  
89 is active in solid tumors in which it correlates with hypoxia and metastasis <sup>19</sup>. However, ISR has not been deeply  
90 studied in leukemia. Since recognized, ISR is proposed as a therapeutic target in cancer <sup>20-22</sup>. Nevertheless, no  
91 efficient and specific strategy has been proposed still, especially for hematological malignancies.

92 We report here that inhibition of ISR signaling by small molecule ISRB combined with imatinib has potential to  
93 eradicate imatinib-resistant CML-BP cells. We show that such treatment specifically changes gene expression  
94 profile and inhibits oncogenic STAT5 signaling. Therefore the combination of ISRB and imatinib was identified as  
95 a possible therapeutic strategy when aiming to eradicate TKI-resistant leukemic cells exhibiting constitutive  
96 STAT5 activation.

97

98

99

100

101 **Methods**

102 **Cell culture**

103 The K562 cells (CCL-243) and LAMA84 cells (CRL-3347) were purchased from American Type Culture Collection  
104 (ATCC) and cultured <sup>13</sup>. Cells were authenticated at ATCC service and were regularly tested for Mycoplasma  
105 contamination. Detailed description of the two-step generation of cells expressing non-phosphorylatable form of  
106 eIF2 $\alpha$  is provided in the Supplementary Information.

107

108 **Isolation of CD34+ CML-BP patient cells**

109 CML CD34+ cells were obtained from the Institute of Hematology and Blood Transfusion in Warsaw, Poland, in  
110 accordance with the Declaration of Helsinki and with patients' consent and approval of the local Ethical  
111 Committee (Ethical and Bioethical Committee UKSW, Approval No.WAW2/059/2019 and WAW2/51/2016,  
112 Approval No. KEiB-19/2017). The characteristics of patient is detailed in the Supplementary Information.  
113 Peripheral blood mononuclear cells (PBMC) were isolated by density gradient centrifugation and CD34+ cells  
114 were separated using EasySep human CD34+ selection cocktail (StemCell Technologies, Inc.). CD34+ cells were  
115 short-term cultured in IMDM medium (Invitrogen) with 10% FBS, 1 ng/ml of granulocyte-macrophage colony-  
116 stimulating factor (GM-CSF), 1 ng/ml of stem cell factor (SCF), 2 ng/ml of interleukin-3 (IL-3). Cells were  
117 cryopreserved and kept in -180C until usage.

118

119 **Cell treatment**

120 Thapsigargin (Sigma) was used at 100 nM; imatinib (gift from Lukasiewicz Pharmaceutical Institute, Warsaw) at  
121 0,5 or 1  $\mu$ M concentrations *in vitro* or at given doses *in vivo*. ISRIB (Merck, SML0843) was given as indicated.  
122 GSK2656157 (GSK157) (Calbiochem) for *in vitro* test was dissolved in DMSO and given as indicated. For *in vivo*  
123 studies, first the step general stock of GSK157 was made (53,3 g of GSK157 to 1523  $\mu$ l DMSO). In the second  
124 step 20  $\mu$ l of the general stock of GSK157 was added to 44  $\mu$ l of PEG400 (MERC, #8074851000) and 40  $\mu$ l of  
125 saline (not PBS).

126

127 ***In vivo* experiments**

128 Experiments were performed using immunodeficient NOD.Cg-PrkdcscidIl2rgtm1WjL/SzJ mice, in accordance with  
129 the Animal Protection Act in Poland (Directive 2010/63/EU) and approved by the Second Local Ethics Committee  
130 (Permission No. WAW/51/2016). Cells ( $10^6$ ) were injected subcutaneously or into tail vain. Mice were treated with:  
131 imatinib - twice a day (50 mg/kg); GSK157 - once a day (20 mg/kg); ISRIB - once a day (2 mg/kg) or in  
132 combination with the same doses, as indicated. Experimental schemes are presented as part of Figures.

133

134 **Flow cytometry**

135 Apoptotic cell death was detected using Annexin V-PE Apoptosis Detection Kit I (BD Biosciences #559763) as  
136 described <sup>13</sup>. To detect phosphorylation of STAT5 and S6K, cells were incubated with eBioscience™ Fixable  
137 Viability Dye eFluor™ 455UV (Thermo Fisher) to discriminate dead cells, followed by staining using Transcription  
138 Factor Phospho Buffer Set (BD Pharmingen) and antibodies: anti-phospho-STAT5 (Tyr694)-PE, and anti-  
139 phospho-S6 (Ser235, Ser236) – eFluor450 (eBioscience, Thermo Fisher). Events were acquired using BD LSR  
140 Fortessa cytometer (Becton Dickinson) and then analysed by FloJo Software (Becton Dickinson).

141

142 **Western Blot**

143 Western blot analysis was performed in a standard conditions, as previously described <sup>13</sup>. List of antibodies is  
144 presented in the Supplementary Information.

145

146 **RT-qPCR analysis**

147 Total RNA was extracted using TRI Reagent (Sigma #T9424) or by Renozol (Genoplast #BMGPB1100-2)  
148 followed by Total RNA Mini column purification kit (A&A Biotechnology #031-100). 2 µg of RNA was subjected to  
149 reverse transcription using M-MLV enzyme (Promega #M1705), dNTP mix 100 mM each (BLIRT #RP65) and  
150 oligo (dT)<sub>18</sub> primers (Bioline #BIO-38029). The RT-qPCR reaction was performed using SensiFAST SYBR Hi-  
151 ROX Kit (Bioline #BIO-92020) on the StepOnePlus™ platform (Thermo Fisher Scientific) according to MIQE  
152 guideline. Primers sequences are listed in the Supplementary Information. The comparative  $2^{-\Delta\Delta Ct}$  method was  
153 used to determine the relative mRNA level using StepOnePlus software. 18SrRNA was used as a reference  
154 control. Data are presented as mean values  $\pm$  SD; n = 3-5). Statistical significance was assessed using unpaired  
155 Student's t-test with Welch's correction and p  $\leq$  0,05 was estimated as significant (\*p  $\leq$  0.05; \*\*p  $\leq$  0.005; \*\*\*p  $\leq$   
156 0.001; \*\*\*\*p  $\leq$  0.0005).

157

158 **RNA Sequencing and data analysis**

159 RNA was isolated as described in RT-qPCR section. The library was prepared using NEB Next Ultra II Directional  
160 RNA library Prep kit for Illumina (#E7335S/L). Sample analysis: the quality of raw data was verified in FASTQ  
161 format from RNA-Seq experiments with FastQC <sup>23</sup>. Because of observed high quality of the raw data, no further  
162 processing of reads was performed. Data analysis was done using the SqulRE <sup>24</sup> pipeline. Human genome hg38  
163 and corresponding refseq gene annotations were downloaded from UCSC (<https://genome.ucsc.edu/>; <sup>25</sup> with  
164 SqulRE. STAR version 2.5.3a <sup>26</sup>, StringTie version 1.3.3b <sup>27</sup>, and DESeq2 version 1.16.1 <sup>28</sup> were used within the  
165 SqulRE pipeline for alignment of reads, transcript assembly and quantification, and differential gene expression  
166 analysis, respectively. Differentially expressed genes with false discovery rate (FDR)  $< 0.05$  were reported here.  
167 Principal component analysis of all samples (11 replicates in total from 4 conditions) based on gene expression

168 data (transcripts per kilobase million or TPM) was performed with <sup>29</sup>. The Clust tool <sup>30</sup> was used for co-expressed  
169 gene clusters identification across all samples. The default normalization procedure of Clust for RNA-seq TPM  
170 data (quantile normalization followed by log2-transformation and Z-score normalization, code “101 3 4”) was  
171 applied. gProfiler <sup>31</sup> was utilized for the simultaneous functional enrichment analysis of the genes from all clusters  
172 in multi-query mode. The RNA-Seq data from this publication have been deposited to the NCBI GEO repository  
173 (<https://www.ncbi.nlm.nih.gov/geo>) and can be accessed with the dataset identifier GSE171853.

174

175 **Statistical analysis**

176 Data were analysed using GraphPad Prism (GraphPad Software, La Jolla, CA, USA) Single comparisons were  
177 tested using unpaired Student’s *t*-tests for normal distributed samples or Mann–Whitney-U tests when normal  
178 distribution was not given. One-way or two-way ANOVA was applied for multiple comparison analysis, with  
179 Bonferroni’s multiple comparison post-test. For RT-qPCR unpaired Student’s *t*-test with Welch’s correction was  
180 applied. P values < 0.05 were estimated as significant (\*p<0.05; \*\*p <0.005; \*\*\*p<0.0005). Data are presented as  
181 mean ± SD.

182

183 **Results**

184 **GENETIC ISR INHIBITION SENSITIZES CML CELLS TO IMATINIB *IN VITRO***

185 To study the impact of Integrated Stress Response globally, ISR was inhibited by targeting the main regulatory  
186 hub - eIF2 $\alpha$ . This was achieved by expression of non-phosphorylatable (S51A) eIF2 $\alpha$  form (visible as additional  
187 band on western blot), followed by overexpression of shRNA against eIF2 $\alpha$  3'UTR (S51A shUTR) to inhibit  
188 expression of endogenous wt eIF2 $\alpha$ , leading altogether to complete lack of eIF2 $\alpha$  phosphorylation (Fig. 1A,  
189 detailed procedure of generation of genetically modified cells is provided in Supplementary Information). Both  
190 generated cell lines had unaffected levels of PERK, an UPR kinase acting upstream of eIF2 $\alpha$ , and expressed  
191 GFP necessary for FACS sorting (Fig. 1A). The functional influence on ISR confirmed by detection of mRNAs  
192 encoding ISR markers *CHOP* and *GADD34* showed that inhibition of the eIF2 $\alpha$  phosphorylation attenuates  
193 dynamics of the ISR activation (Fig. S1A). In addition, inhibition of the eIF2 $\alpha$  phosphorylation itself decreased cell  
194 viability (Fig. 1B), and associated with increased basal *GADD34* and *CHOP* mRNA levels indicating stress-  
195 induced cell death (Fig. S1B). This indicated that the lack of ISR pathway itself is cytotoxic for CML cells.  
196 Furthermore, imatinib-induced apoptosis was higher in S51A and further increased in S51A shUTR cells,  
197 compared to wt (Fig. 1C). This implies that indeed K562 cells utilize the eIF2 $\alpha$  phosphorylation-dependent  
198 mechanism and that ISR inhibition sensitizes CML cells to imatinib.

199 **ISRB, BUT NOT GSK157, SENSITIZES CML CELLS TO IMATINIB *IN VIVO***

200 Even if the genetic approaches are useful, the pharmacological inhibition still gives the highest possibility for the  
201 clinical applications targeting the signaling pathways. Thus, we tested two ISR inhibitors: GSK2656157 (GSK157)  
202 and ISRB (Fig. 2A). GSK157 is an ATP-competitive inhibitor of PERK kinase, which stops the PERK-dependent  
203 ISR activation. Small molecule ISRB blocks the eIF2 $\alpha$ -P-dependent downstream signaling and inhibits the  
204 executive part of ISR, without the cytotoxic effects<sup>32-35</sup>. Both drugs have not been tested in leukemia, including  
205 CML. Pre-conditioning of K562 CML cells with either GSK157 or ISRB, followed by ISR induction by thapsigargin,  
206 revealed that both ISR inhibitors significantly reduced expression of *CHOP* and *GADD34* mRNAs in leukemia  
207 cells (Fig. 2B, C).

208 The results obtained *in vitro* (Fig. 2) imply that ISR inhibitors might improve the imatinib efficacy and eliminate  
209 CML cells. To test this hypothesis and verify cell survival and growth potential *in vivo*, xenograft studies were  
210 performed using NSG immunodeficient mice and GFP+ K562 cells (experimental scheme and treatment - Fig.  
211 3A). After the time period necessary for leukemia cells growth, tumors were found in all untreated mice.  
212 Remarkably, only combination of imatinib and ISRB significantly decreased number of animals with tumors (41%  
213 of mice developed tumors) (Fig. 3B). This was associated with the decreased tumor mass by more than 70% (Fig.  
214 3C, D). Conversely, imatinib or imatinib with GSK157 exerted only moderate inhibitory effect, and the average  
215 tumour mass was not significantly different between those conditions. These results show that ISRB but not  
216 GSK157 sensitizes CML to imatinib *in vivo*.

217

218 **ISRB COMBINED WITH IMATINIB ATTENUATES ENGRAFTMENT OF PRIMARY TKI-REFRACTORY CML  
219 CD34+ BLASTS**

220 Since the results in Fig. 3 implicated that combination of ISRB and imatinib might eradicate imatinib-resistant  
221 CML cells and decrease the leukemia development, it was of paramount importance to verify this in the PDX  
222 model using NSG mice as a host bearing CD34+ CML cells resistant to imatinib and dasatinib. CD34+ cells were  
223 isolated from patient diagnosed in Blast Phase (BP), who initially responded to high dose imatinib, but  
224 subsequently developed resistance to imatinib, despite lack of detected (at the time of resistance) mutations  
225 within the kinase domain of BCR-ABL1. Dasatinib was introduced, but yielded only a transient effect. Next-  
226 generation sequencing revealed pathogenic variant in *PTPN11* gene described in hematological malignancies  
227<sup>36,37</sup>. The detailed patient characteristics are provided in the Supplementary Information. *PTPN11* gain-of-function  
228 mutations result in overactivation of the RAS/RAF/MAPK/ERK and the JAK/STAT pathways, in addition to their  
229 possible activation caused by BCR-ABL1. Thus, such cells represent a BCR-ABL1-independent, imatinib/TKI  
230 resistant phenotype.

231 A short and aggressive 7-day regimen was applied to test the beneficial effects, followed by treatment with  
232 imatinib or ISRIB alone or with drug combination (experimental scheme - Fig. 4A). All variants showed noticeable  
233 but not significant decrease in the spleen weight (Fig. 4B). To estimate the short-term engraftment, the  
234 percentage of human CD45+ (hCD45+) was detected within the bone marrow or spleen populations (Fig. 4C, 4D,  
235 4E; Fig. S2). Combination of imatinib and ISRIB significantly decreased percentage of hCD45+ cells in the bone  
236 marrow, showing a 2- to 3-fold lower level compared to the treatment with imatinib or ISRIB alone. In addition, the  
237 combined treatment treatment decreased the engraftment into the spleen (which is considered as a secondary  
238 niche), compared to imatinib alone (Fig. 4E). These results showed that the combined treatment eradicates  
239 resistant blasts and decreases leukemia engraftment, therefore confirming the synergistic effect of imatinib and  
240 ISRIB.

241

242 **COMBINATION OF ISRIB AND IMATINIB REPROGRAMMES THE GENE EXPRESSION PROFILE OF**  
243 **PRIMARY TKI-RESISTANT BLASTS**

244 To investigate the molecular effects of the double treatment, RNA-seq was performed on FACS-sorted hCD45+  
245 CML cells isolated from the PDX bone marrow. Principal component analysis (PCA) indicated that cells treated  
246 with imatinib and ISRIB are transcriptionally distinct (Fig. 5A). This was confirmed by hierarchical clustering of  
247 significantly changed genes between pairs of tested conditions (treatment vs control), and supported by the  
248 Pearson correlation values, which showed higher correlation between sole ISRIB and sole imatinib treatment  
249 compared to control ( $r = 0.69$ ), than between each of the single treatments and the combined imatinib+ISRIB  
250 treatment compared to control ( $r = 0.32$  and  $0.37$ , respectively; Fig. 5B). The *SGK3* and *SNURF/SNRPN* genes  
251 regulating alternative RNA processing were identified as significantly downregulated upon the double treatment.  
252 Upregulated genes in majority encoded proteins regulating transcription and RNA processing.

253 To identify genes responsible for the increased sensitivity, the gene expression profiles for imatinib versus  
254 imatinib + ISRIB were compared. In addition to the previously described (Fig. 5B), genes encoding proteins from  
255 the small GTP-binding RAS superfamily (*RGPD5* and *RGPD8*) were significantly downregulated (Fig. 5C, for all  
256 treatment combinations see Fig. S3A).

257 Since genes that are co-expressed are often co-regulated, clusters of co-expressed genes (C0-C12) across all  
258 variants of treatment were identified (all genes included, regardless of their statistical significance of change in  
259 expression) (Fig. 5D). Clusters with the highest number of genes represented the groups in which drug  
260 combination led to either sharp decrease (C0, C1) or increase (C5, C6) of gene expression (Fig. 5D, 5E). Those  
261 four clusters represented about 72% of all detected genes (Fig. 5E). This clearly indicated that the gene  
262 expression pattern for ISRIB + imatinib combination is specific and different from the other treatment conditions.

263

264 **COMBINATION OF IMATINIB AND ISRIB DOWNREGULATES GENES RELATED TO PROLEUKEMIC  
265 SIGNALING**

266 To predict the cellular mechanisms altered by combined treatment, all 13 defined gene clusters underwent the  
267 functional enrichment analysis. The C0 and C1 clusters which included genes downregulated upon combined  
268 treatment, were significantly enriched in terms related to RAS/RAF/BRAF/MAPK signalling (Fig. 6, marked in red,  
269 and Fig S5; for all clusters see Fig. S3). Specifically, for Ras and MAPK signaling (detailed member genes in Fig.  
270 S4A, S4B), genes encoding RAF1, ARAF, ERK2, KRAS, SRC, JAK2 and a number of proteins involved in  
271 activation of MAPK cascade such as: MEK1, MAPK1, MAP4K1, MAP3K3, MADD were downregulated upon  
272 combined treatment. The drug combination attenuated also IFN $\gamma$  signalling and immune response, which in  
273 leukemia can additionally mediate activation of the JAK2/STAT5 pathway and inflammatory response (Fig. 6,  
274 marked in blue; for all clusters see Fig. S3B). Downregulation of processes essential for leukemia-promoting  
275 kinase-dependent signaling and immune response was also confirmed by Gene Ontology Biological Processes  
276 (BP) terms (Fig. S5, see C0 and C1 clusters).

277 While SGK3 gene encoding serine/threonine-protein kinase SGK3 was significantly downregulated after the  
278 combined treatment (Fig. 5B), expression of the SGK3 interaction partners, selected based on the interaction  
279 partner datasource: BioGRID, IntAct (EMBL-EBI) and APID databases (see Supplementary Information), showed  
280 rather moderate inhibition upon combined treatment (Fig. S6). Among the downregulated genes, we found  
281 GSK3 $\beta$ , what may suggest its regulatory connection with SGK3 and specific downregulation upon combined  
282 treatment.

283 Altogether, these results showed that genes related to oncogenic pro-leukemic signaling were downregulated  
284 upon combination of imatinib and ISRIB, presumably enhancing targeting of leukemia cells by imatinib.

285

286 **COMBINATION OF ISRIB AND IMATINIB INHIBITS STAT5 SIGNALING IN CML CELLS**

287 Transcriptomic data indicated that the combined treatment can downregulate oncogenic RAS/RAF/MAPK, JAK2,  
288 SGK3 and IFN $\gamma$  signalling. In addition, genes that are mediators of JAK2/STAT5 signalling were attenuated (Fig.  
289 6, Fig. S4, S5). This indicated that the combined treatment might inhibit the STAT5 pathway.

290 To obtain direct evidence that treatment with imatinib + ISRIB shows synergistic effect, STAT5 phosphorylation  
291 was assessed in K562 and LAMA84 cell lines, which were shown to activate the above signaling pathways <sup>13,38</sup>.  
292 To better visualize the effects, strong ISR response *in vitro* was activated by thapsigargin. In both cell lines,  
293 combination of ISRIB with imatinib decreased STAT5 phosphorylation detected by western blot (Fig. 7A, 7B), and  
294 confirmed by phospho- flow cytometry (Fig. 7C). On the other hand, ISRIB alone did not change, whereas  
295 imatinib alone only partially decreased phosphorylation of STAT5, compared to double treatment, with effectivity

296 lower in K562 cells, which were more resistant. Conversely, the significant additive effect (estimated by the  
297 phosphorylation levels) of the combined therapy combined to imatinib alone was not observed for other pro-  
298 leukemic related regulators such as: AKT, mTOR, S6K, SGK3, GSK3 $\beta$  or ERK (Fig. S7). So, the genetic data  
299 indicating downregulation of the SGK3 - GSK3 $\beta$  link were not confirmed *in vitro*. Interestingly, inhibition of AKT  
300 and ERK phosphorylation by imatinib (Fig. S7A and S7F, respectively), associated with decreased BCR-ABL1  
301 activity (Fig. S8A), but not BCR-ABL1 protein level (Fig. S8B), indicated that either pAKT or pERK are not  
302 involved in acquiring the BCR-ABL1-independent resistance.

303 The results presented in Fig. 7A-7D imply that the combined treatment attenuates the STAT5-dependent  
304 signaling. To test this, the fold change analysis of the STAT5 target genes expression was performed within the  
305 C0 and C1 clusters (downregulated upon imatinib + ISRIB). The list of possible STAT5 target genes was created  
306 based on ChIP-Seq data from malignant/hematopoietic cells (see Supplementary Information). As expected, the  
307 combined treatment decreased expression of STAT5 target genes (*SSH2*, *CCND3*, *MAP3K5*, *SGK1*, *DOCK8*,  
308 *DUSP1* and *HBEGF*), compared to control or single treatments (Fig. 7E, 7F). Negatively regulated STAT5-target  
309 genes encoded regulators of cell cycle/proliferation, stress response and survival, including Slingshot Protein  
310 Phosphatase, Cyclin D3, ZIR8, MAP kinase phosphatase 1, EGF-like growth factor, MAP3K5 and SGK1. Data for  
311 all clusters are presented in Fig. S9. Conversely, such inhibitory effect was not observed for imatinib and ISRIB  
312 alone. Altogether, obtained data clearly support the conclusion that combination of imatinib and ISRIB shows the  
313 substantial synergistic effect and inhibits the proleukemic STAT5 signaling in CML-BC TKIs resistant cells.

314

## 315 **Discussion**

316 Development of imatinib has revolutionised CML treatment and patients' overall survival. Despite the clinical  
317 success of imatinib in the CML-CP treatment, the disease is still not fully curable and eradication of all leukemic  
318 cells is not efficient. Imatinib intolerance or primary resistance occurs, as well as many patients develop  
319 secondary resistance due to activation of signaling pathways, including JAK/STAT5, GSK3 $\beta$  or RAS/MEK/ERK  
320 <sup>3,8,9</sup>. Importantly, such activation might occur in a BCR-ABL1-independent manner, thus upon imatinib treatment  
321 of even BCR-ABL1 non-mutated cells, those oncogenic pathways still remain active. Therefore, one of the current  
322 strategies to eradicate leukemic blasts, is to target BCR-ABL1 together with oncogenic signaling pathways, to  
323 resensitize cells to TKIs <sup>5,39-41</sup>.

324 Here we provide evidence that inhibition of Integrated Stress Response by ISRIB combined together with imatinib  
325 might significantly break the resistance by targeting both, the stress response adaptative signaling as well as the  
326 STAT5-dependent intrinsic signaling. This can result in effective elimination of imatinib-refractory cells in CML.  
327 Unexpectedly, only ISRIB but not another ISR inhibitor - GSK157 belonging to the PERK inhibitors family, was  
328 effective *in vivo*. This is consistent with recent studies of amyotrophic lateral sclerosis which showed similar data

329 indicating that ISRIB but not GSK157 inhibitor, was more effective and improved neuronal survival <sup>42</sup>. Such effect  
330 can be a result of an eIF2 $\alpha$  phosphorylation-independent effects <sup>43</sup>, moderate specificity of GSK157, as its affinity  
331 to RIPK1 was shown to be significantly higher than to PERK kinase <sup>44</sup>, as well as the pancreatic toxicity reported  
332 recently <sup>45</sup>. Moreover, as PERK inhibitors target only one of four ISR arms, it can not be neglected that another  
333 parallel signaling leading to ISR is still active *in vivo*. In addition, ISRIB may have other, yet undescribed, targets.  
334 Results presented here provided several possible signaling pathways which may be altered by ISRIB in malignant  
335 cells.

336 ISRIB molecule, discovered in 2013, in contrast to PERK inhibitors, acts below eIF2 $\alpha$  and directly reverses  
337 attenuation of the eIF2B by phosphorylated eIF2 $\alpha$  <sup>33,46,47</sup>. ISRIB has been proposed as a promising drug in the  
338 brain malignant conditions and age-related memory decline <sup>48,49</sup>, as well as in some metastatic tumours <sup>50,51,52,53</sup>.  
339 Recent studies showed that chemotherapy combined with ISRIB abrogates breast cancer plasticity and improves  
340 the therapeutic efficacy <sup>19</sup>. This observation strongly supports the statement presented here. Studies of the clinical  
341 potential of ISRIB in hematological malignancies are limited <sup>54,55</sup>. This study is the first to show ISRIB  
342 effectiveness in a combined therapy against CML-BP TKI-resistant blasts.

343 Mechanistically, we have discovered that the combined treatment inhibits STAT5 phosphorylation and decreases  
344 expression of STAT5 target genes, that regulate proliferation, apoptosis and stress response. Targeting STAT5,  
345 which is an oncogenic signaling in imatinib resistant forms of CML <sup>3,9,56</sup>, effectively overcomes resistance and  
346 eradicates leukemic cells <sup>57-59</sup>. The experimental therapy proposed by us, not only inhibits ISR but also attenuates  
347 the STAT5-dependent signaling in CML. It is to note, that the overactivated STAT5 has also been detected in  
348 other hematopoietic malignancies, such as non-CML chronic myeloproliferative disorders correlating with JAK2  
349 V617F mutation <sup>60</sup> or Flt3-ITD positive AML <sup>61</sup>. Therefore, it is worth considering that the proposed strategy might  
350 be effective also in other blood disorders.

351 In striking contrast, even if downregulation of related genes was observed in the transcriptomic analysis, the  
352 mTOR, SGK3, GSK3 $\beta$ , AKT and ERK activity was not specifically targeted by the double treatment *in vitro*.  
353 Notably, even though the regulatory ISR-SGK3 link was shown in glioma <sup>62</sup>, and our transcriptomic data indicated  
354 SGK3 downregulation by the combined treatment, this was not confirmed in the model studies *in vitro*. On the  
355 other hand, pAKT and pERK, together with BCR-ABL1 activity were inhibited already by imatinib alone, and not  
356 further downregulated by drug combination. Therefore, those pathways were probably not responsible for the  
357 resistant phenotype. Nevertheless, in other leukemias in which the resistance developed due to AKT or ERK  
358 overactivation, such effect might help to eradicate the resistant blasts.

359 Interestingly, differential expression of genes responsible for the immune modulation (visible even in the xenograft  
360 model, which excludes involvement of T and B lymphocytes, but still encompasses functional myeloid cells)  
361 suggests possible involvement of the immune system remodelling in the therapeutic outcome. This data support  
362 the idea of targeting the innate immune system or immune checkpoints in myeloid malignancies, including CML

363 <sup>63–65</sup>. Thus, even though experiments were performed in immunodeficient (lacking adaptive, lymphocyte-mediated  
364 response) mice, signaling and functional effects related to the innate immune responses (mediated by e.g.  
365 macrophages) were possibly functional leading to the observed changes. Although interesting, this has to be  
366 verified in subsequent studies using the syngenic mouse model.

367 In conclusion, we discovered a novel strategy to break the resistance and eradicate imatinib-refractory CML  
368 blasts, which is based on therapeutic combination of ISR inhibitor ISRib together with imatinib. We postulate that  
369 such strategy can improve therapeutic outcomes in CML patients showing TKI resistance related to overactivated  
370 STAT5 and stress adaptation signaling. Possibly, a similar approach based on ISRib combined with a typical  
371 chemotherapy may also be applied to other hematological malignancies with constitutively activated STAT5  
372 signaling and STAT5-dependent resistance.

373

374 **Acknowledgements**

375 The research was funded by National Science Centre grants: PRELUDIUM (2015/19/N/NZ3/02267) to WD,  
376 Sonata Bis (2013/10/E/NZ3/00673) to KP and HARMONIA (2014/14/M/NZ5/00441) to TS. KP was also supported  
377 by TEAM-TECH Core Facility Plus (POIR.04.04.00-00-23C2/17-00) grant from Foundation for Polish Science co-  
378 financed by the European Union under the European Regional Development Fund. Authors would like to thank  
379 Dr. Antonis E. Koromilas for providing non-phosphorylatable eIF2 $\alpha$  S51A mutated form of eIF2 $\alpha$  and valuable  
380 discussions, Lukasz Bugajski for help with part of experiments by FACS sorting, Danuta Wasilewska and  
381 Zuzanna Sipak for animal breeding and tissue isolation, and Jelena Pistolic and Vladimir Benes for help with RNA  
382 Seq library sample preparation. RNA Seq analyses were performed at the Gene Core EMBL Laboratory in  
383 Heidelberg.

384

385 **Competing Interests statement**

386 The authors declare no competing financial interests.

387

388

389

390

391

392

393

394

395

396 **References**

397 1 Eiring AM, Khorashad JS, Morley K, Deininger MW. Advances in the treatment of chronic myeloid leukemia.  
398 *BMC Med* 2011; **9**: 99.

399 2 Iqbal N, Iqbal N. Imatinib: a breakthrough of targeted therapy in cancer. *Chemother Res Pract* 2014; **2014**:  
400 357027.

401 3 Braun TP, Eide CA, Druker BJ. Response and Resistance to BCR-ABL1-Targeted Therapies. *Cancer Cell*  
402 2020; **37**: 530–542.

403 4 Perrotti D, Jamieson C, Goldman J, Skorski T. Chronic myeloid leukemia: mechanisms of blastic  
404 transformation. *J Clin Invest* 2010; **120**: 2254–2264.

405 5 Soverini S, Mancini M, Bavaro L, Cavo M, Martinelli G. Chronic myeloid leukemia: the paradigm of targeting  
406 oncogenic tyrosine kinase signaling and counteracting resistance for successful cancer therapy. *Mol Cancer*  
407 2018; **17**: 49.

408 6 Chien S-H, Liu H-M, Chen P-M, Ko P-S, Lin J-S, Chen Y-J *et al.* The landscape of BCR-ABL mutations in  
409 patients with Philadelphia chromosome-positive leukaemias in the era of second-generation tyrosine kinase  
410 inhibitors. *Hematol Oncol* 2020; **38**: 390–398.

411 7 Soverini S, De Benedittis C, Papayannidis C, Paolini S, Venturi C, Iacobucci I *et al.* Drug resistance and  
412 BCR-ABL kinase domain mutations in Philadelphia chromosome-positive acute lymphoblastic leukemia from  
413 the imatinib to the second-generation tyrosine kinase inhibitor era: The main changes are in the type of  
414 mutations, but not in the frequency of mutation involvement. *Cancer* 2014; **120**: 1002–1009.

415 8 Steelman LS, Pohnert SC, Shelton JG, Franklin RA, Bertrand FE, McCubrey JA. JAK/STAT, Raf/MEK/ERK,  
416 PI3K/Akt and BCR-ABL in cell cycle progression and leukemogenesis. *Leukemia* 2004; **18**: 189–218.

417 9 Warsch W, Grundschober E, Sexl V. Adding a new facet to STAT5 in CML: multitasking for leukemic cells.  
418 *Cell Cycle Georget Tex* 2013; **12**: 1813–1814.

419 10 Bertacchini J, Heidari N, Mediani L, Capitani S, Shahjahani M, Ahmadzadeh A *et al.* Targeting  
420 PI3K/AKT/mTOR network for treatment of leukemia. *Cell Mol Life Sci CMLS* 2015; **72**: 2337–2347.

421 11 Hantschel O. Targeting BCR-ABL and JAK2 in Ph+ ALL. *Blood* 2015; **125**: 1362–1363.

422 12 Lernoux M, Schnekenburger M, Losson H, Vermeulen K, Hahn H, Gérard D *et al.* Novel HDAC inhibitor  
423 MAKV-8 and imatinib synergistically kill chronic myeloid leukemia cells via inhibition of BCR-ABL/MYC-  
424 signaling: effect on imatinib resistance and stem cells. *Clin Epigenetics* 2020; **12**: 69.

425 13 Kusio-Kobialka M, Podsywalow-Bartnicka P, Peidis P, Glodkowska-Mrowka E, Wolanin K, Leszak G *et al.*  
426 The PERK-eIF2 $\alpha$  phosphorylation arm is a pro-survival pathway of BCR-ABL signaling and confers  
427 resistance to imatinib treatment in chronic myeloid leukemia cells. *Cell Cycle Georget Tex* 2012; **11**: 4069–  
428 4078.

429 14 Nguyen HG, Conn CS, Kye Y, Xue L, Forester CM, Cowan JE *et al.* Development of a stress response  
430 therapy targeting aggressive prostate cancer. *Sci Transl Med* 2018; **10**. doi:10.1126/scitranslmed.aar2036.

431 15 Salminen A, Kaarniranta K, Kauppinen A. Integrated stress response stimulates FGF21 expression:  
432 Systemic enhancer of longevity. *Cell Signal* 2017; **40**: 10–21.

433 16 van Galen P, Mbong N, Kreso A, Schoof EM, Wagenblast E, Ng SWK *et al.* Integrated Stress Response  
434 Activity Marks Stem Cells in Normal Hematopoiesis and Leukemia. *Cell Rep* 2018; **25**: 1109-1117.e5.

435 17 Wang C, Tan Z, Niu B, Tsang KY, Tai A, Chan WCW *et al.* Inhibiting the integrated stress response pathway  
436 prevents aberrant chondrocyte differentiation thereby alleviating chondrodysplasia. *eLife* 2018; **7**.  
437 doi:10.7554/eLife.37673.

438 18 Ron D, Walter P. Signal integration in the endoplasmic reticulum unfolded protein response. *Nat Rev Mol  
439 Cell Biol* 2007; **8**: 519–529.

440 19 Jewer M, Lee L, Leibovitch M, Zhang G, Liu J, Findlay SD *et al.* Translational control of breast cancer  
441 plasticity. *Nat Commun* 2020; **11**: 2498.

442 20 Darini C, Ghaddar N, Chabot C, Assaker G, Sabri S, Wang S *et al.* An integrated stress response via PKR  
443 suppresses HER2+ cancers and improves trastuzumab therapy. *Nat Commun* 2019; **10**: 2139.

444 21 Atkins C, Liu Q, Minthorn E, Zhang S-Y, Figueroa DJ, Moss K *et al.* Characterization of a novel PERK kinase  
445 inhibitor with antitumor and antiangiogenic activity. *Cancer Res* 2013; **73**: 1993–2002.

446 22 Sidrauski C, McGeachy AM, Ingolia NT, Walter P. The small molecule ISRIB reverses the effects of eIF2 $\alpha$   
447 phosphorylation on translation and stress granule assembly. *eLife* 2015; **4**: e05033.

448 23 Babraham Bioinformatics - FastQC A Quality Control tool for High Throughput Sequence Data.  
449 <http://www.bioinformatics.babraham.ac.uk/projects/fastqc/> (accessed 30 Aug2020).

450 24 Yang WR, Ardeljan D, Pacyna CN, Payer LM, Burns KH. SQuIRE reveals locus-specific regulation of  
451 interspersed repeat expression. *Nucleic Acids Res* 2019; **47**: e27.

452 25 Haeussler M, Zweig AS, Tyner C, Speir ML, Rosenbloom KR, Raney BJ *et al.* The UCSC Genome Browser  
453 database: 2019 update. *Nucleic Acids Res* 2019; **47**: D853–D858.

454 26 Dobin A, Davis CA, Schlesinger F, Drenkow J, Zaleski C, Jha S *et al.* STAR: ultrafast universal RNA-seq  
455 aligner. *Bioinforma Oxf Engl* 2013; **29**: 15–21.

456 27 Pertea M, Pertea GM, Antonescu CM, Chang T-C, Mendell JT, Salzberg SL. StringTie enables improved  
457 reconstruction of a transcriptome from RNA-seq reads. *Nat Biotechnol* 2015; **33**: 290–295.

458 28 Love MI, Huber W, Anders S. Moderated estimation of fold change and dispersion for RNA-seq data with  
459 DESeq2. *Genome Biol* 2014; **15**: 550.

460 29 Pedregosa F, Varoquaux G, Gramfort A, Michel V, Thirion B, Grisel O *et al.* Scikit-learn: Machine Learning in  
461 Python. *J Mach Learn Res* 2011; **12**: 2825–2830.

462 30 Abu-Jamous B, Kelly S. Clust: automatic extraction of optimal co-expressed gene clusters from gene  
463 expression data. *Genome Biol* 2018; **19**: 172.

464 31 Reimand J, Arak T, Adler P, Kolberg L, Reisberg S, Peterson H *et al.* g:Profiler-a web server for functional  
465 interpretation of gene lists (2016 update). *Nucleic Acids Res* 2016; **44**: W83-89.

466 32 Halliday M, Radford H, Sekine Y, Moreno J, Verity N, le Quesne J *et al.* Partial restoration of protein  
467 synthesis rates by the small molecule ISRIB prevents neurodegeneration without pancreatic toxicity. *Cell  
468 Death Dis* 2015; **6**: e1672.

469 33 Sidrauski C, Acosta-Alvear D, Khoutorsky A, Vedantham P, Hearn BR, Li H *et al.* Pharmacological brake-  
470 release of mRNA translation enhances cognitive memory. *eLife* 2013; **2**: e00498.

471 34 Wong YL, LeBon L, Basso AM, Kohlhaas KL, Nikkel AL, Robb HM *et al.* eIF2B activator prevents  
472 neurological defects caused by a chronic integrated stress response. *eLife* 2019; **8**: e42940.

473 35 Wong YL, LeBon L, Edalji R, Lim HB, Sun C, Sidrauski C. The small molecule ISRIB rescues the stability  
474 and activity of Vanishing White Matter Disease eIF2B mutant complexes. *eLife* 2018; **7**.  
475 doi:10.7554/eLife.32733.

476 36 Tartaglia M, Niemeyer CM, Fragale A, Song X, Buechner J, Jung A *et al.* Somatic mutations in PTPN11 in  
477 juvenile myelomonocytic leukemia, myelodysplastic syndromes and acute myeloid leukemia. *Nat Genet*  
478 2003; **34**: 148–150.

479 37 Xu R, Yu Y, Zheng S, Zhao X, Dong Q, He Z *et al.* Overexpression of Shp2 tyrosine phosphatase is  
480 implicated in leukemogenesis in adult human leukemia. *Blood* 2005; **106**: 3142–3149.

481 38 Sonoyama J, Matsumura I, Ezoe S, Satoh Y, Zhang X, Kataoka Y *et al.* Functional cooperation among Ras,  
482 STAT5, and phosphatidylinositol 3-kinase is required for full oncogenic activities of BCR/ABL in K562 cells. *J  
483 Biol Chem* 2002; **277**: 8076–8082.

484 39 Agarwal P, Zhang B, Ho Y, Cook A, Li L, Mikhail FM *et al.* Enhanced targeting of CML stem and progenitor  
485 cells by inhibition of porcupine acyltransferase in combination with TKI. *Blood* 2017; **129**: 1008–1020.

486 40 Merchant AA, Matsui W. Targeting Hedgehog--a cancer stem cell pathway. *Clin Cancer Res Off J Am Assoc  
487 Cancer Res* 2010; **16**: 3130–3140.

488 41 Tusa I, Cheloni G, Poteti M, Gozzini A, DeSouza NH, Shan Y *et al.* Targeting the Extracellular Signal-  
489 Regulated Kinase 5 Pathway to Suppress Human Chronic Myeloid Leukemia Stem Cells. *Stem Cell Rep*  
490 2018; **11**: 929–943.

491 42 Bugallo R, Marlin E, Baltanás A, Toledo E, Ferrero R, Vinuela-Gavilanes R *et al.* Fine tuning of the unfolded  
492 protein response by ISRIB improves neuronal survival in a model of amyotrophic lateral sclerosis. *Cell Death  
493 Dis* 2020; **11**: 397.

494 43 Krishnamoorthy J, Rajesh K, Mirzajani F, Kesoglidiou P, Papadakis AI, Koromilas AE. Evidence for eIF2α  
495 phosphorylation-independent effects of GSK2656157, a novel catalytic inhibitor of PERK with clinical  
496 implications. *Cell Cycle* 2014; **13**: 801-806

497 44. Rojas-Rivera D, Delvaeye T, Roelandt R, Nerinckx W, Augustyns K, Vandenabeele P *et al.* When PERK  
498 inhibitors turn out to be new potent RIPK1 inhibitors: critical issues on the specificity and use of GSK2606414  
499 and GSK2656157. *Cell Death Differ* 2017; **24**: 1100–1110.

500 45 Hughes DT, Halliday M, Smith HL, Verity NC, Molloy C, Radford H *et al.* Targeting the kinase insert loop of  
501 PERK selectively modulates PERK signaling without systemic toxicity in mice. *Sci Signal* 2020; **13**.  
502 doi:10.1126/scisignal.abb4749.

503 46 Zyryanova AF, Kashiwagi K, Rato C, Harding HP, Crespillo-Casado A, Perera LA *et al.* ISRB Blunts the  
504 Integrated Stress Response by Allosterically Antagonising the Inhibitory Effect of Phosphorylated eIF2 on  
505 eIF2B. *Mol Cell* 2021; **81**: 88-103.e6.

506 47 Zyryanova AF, Weis F, Faille A, Alard AA, Crespillo-Casado A, Sekine Y *et al.* Binding of ISRB reveals a  
507 regulatory site in the nucleotide exchange factor eIF2B. *Science* 2018; **359**: 1533–1536.

508 48 Costa-Mattioli M, Walter P. The integrated stress response: From mechanism to disease. *Science* 2020; **368**.  
509 doi:10.1126/science.aat5314.

510 49 Krukowski K, Nolan A, Frias ES, Boone M, Ureta G, Grue K *et al.* Small molecule cognitive enhancer  
511 reverses age-related memory decline in mice. *eLife* 2020; **9**. doi:10.7554/eLife.62048.

512 50 Nguyen HG, Conn CS, Kye Y, Xue L, Forester CM, Cowan JE *et al.* Development of a stress response  
513 therapy targeting aggressive prostate cancer. *Sci Transl Med* 2018; **10**. doi:10.1126/scitranslmed.aar2036.

514 51 Palam LR, Gore J, Craven KE, Wilson JL, Korc M. Integrated stress response is critical for gemcitabine  
515 resistance in pancreatic ductal adenocarcinoma. *Cell Death Dis* 2015; **6**: e1913.

516 52 Markouli M, Strepkos D, Papavassiliou AG, Piperi C. Targeting of endoplasmic reticulum (ER) stress in  
517 gliomas. *Pharmacol Res* 2020; **157**: 104823.

518 53 Mahameed M, Boukeileh S, Obiedat A, Darawshi O, Dipta P, Rimon A *et al.* Pharmacological induction of  
519 selective endoplasmic reticulum retention as a strategy for cancer therapy. *Nat Commun* 2020; **11**: 1304.

520 54 Mazurkiewicz M, Hillert E-K, Wang X, Pellegrini P, Olofsson MH, Selvaraju K *et al.* Acute lymphoblastic  
521 leukemia cells are sensitive to disturbances in protein homeostasis induced by proteasome deubiquitinase  
522 inhibition. *Oncotarget* 2017; **8**: 21115–21127.

523 55 Williams MS, Amaral FM, Simeoni F, Somervaille TC. A stress-responsive enhancer induces dynamic drug  
524 resistance in acute myeloid leukemia. *J Clin Invest* 2020; **130**: 1217–1232.

525 56 Hamilton A, Helgason GV, Schemionek M, Zhang B, Myssina S, Allan EK *et al.* Chronic myeloid leukemia  
526 stem cells are not dependent on Bcr-Abl kinase activity for their survival. *Blood* 2012; **119**: 1501–1510.

527 57 Martín-Rodríguez P, Guerra B, Hueso-Falcón I, Aranda-Tavío H, Díaz-Chico J, Quintana J *et al.* A Novel  
528 Naphthoquinone-Coumarin Hybrid That Inhibits BCR-ABL1-STAT5 Oncogenic Pathway and Reduces  
529 Survival in Imatinib-Resistant Chronic Myelogenous Leukemia Cells. *Front Pharmacol* 2018; **9**: 1546.

530 58 Nelson EA, Walker SR, Weisberg E, Bar-Natan M, Barrett R, Gashin LB *et al.* The STAT5 inhibitor pimozide  
531 decreases survival of chronic myelogenous leukemia cells resistant to kinase inhibitors. *Blood* 2011; **117**:  
532 3421–3429.

533 59 Toda J, Ichii M, Oritani K, Shibayama H, Tanimura A, Saito H *et al.* Signal-transducing adapter protein-1 is  
534 required for maintenance of leukemic stem cells in CML. *Oncogene* 2020; **39**: 5601–5615.

535 60 Aboudola S, Murugesan G, Szpurka H, Ramsingh G, Zhao X, Prescott N *et al.* Bone marrow phospho-  
536 STAT5 expression in non-CML chronic myeloproliferative disorders correlates with JAK2 V617F mutation  
537 and provides evidence of in vivo JAK2 activation. *Am J Surg Pathol* 2007; **31**: 233–239.

538 61 Wingelhofer B, Maurer B, Heyes EC, Cumaraswamy AA, Berger-Becvar A, de Araujo ED *et al.*  
539 Pharmacologic inhibition of STAT5 in acute myeloid leukemia. *Leukemia* 2018; **32**: 1135–1146.

540 62 Minchenko DO, Riabovol OO, Tsymbal DO, Ratushna OO, Minchenko OH. Inhibition of IRE1 signaling  
541 affects the expression of genes encoded glucocorticoid receptor and some related factors and their hypoxic  
542 regulation in U87 glioma cells. *Endocr Regul* 2016; **50**: 127–136.

543 63 Arruga F, Gyau BB, Iannello A, Vitale N, Vaisitti T, Deaglio S. Immune Response Dysfunction in Chronic  
544 Lymphocytic Leukemia: Dissecting Molecular Mechanisms and Microenvironmental Conditions. *Int J Mol Sci*  
545 2020; **21**. doi:10.3390/ijms21051825.

546 64 Chao MP, Takimoto CH, Feng DD, McKenna K, Gip P, Liu J *et al.* Therapeutic Targeting of the Macrophage  
547 Immune Checkpoint CD47 in Myeloid Malignancies. *Front Oncol* 2019; **9**: 1380.

548 65 Curran E, Corrales L, Kline J. Targeting the innate immune system as immunotherapy for acute myeloid  
549 leukemia. *Front Oncol* 2015; **5**: 83.

550 66 Jassal B, Matthews L, Viteri G, Gong C, Lorente P, Fabregat A *et al.* The reactome pathway knowledgebase.  
551 *Nucleic Acids Res* 2020; **48**: D498–D503.

552

553

554 **Figure Legends**

555

556 **Figure 1. Genetic ISR inhibition by targeting eIF2 $\alpha$  phosphorylation increases apoptosis induction and**  
557 **sensitizes K562 CML cells to imatinib *in vitro*.**

558 A. Left panel: transfection levels estimated by GFP fluorescence detection by flow cytometry. Overlay of  
559 representative histograms of K562 CML cells expressing wt eIF2 $\alpha$  (green line), mutated non-phosphorylatable form  
560 eIF2 $\alpha$ S51A (orange line) and mutated form together with construct containing shRNA sequence against 3'UTR  
561 region of eIF2 $\alpha$  (S51A shUTR – red line); Right panel: The levels of PERK, eIF2 $\alpha$  and phosphorylated  
562 eIF2 $\alpha$  (S51P) protein estimated by western blot in wt, or stably transfected eIF2 $\alpha$ S51A and S51A shUTR mutants.  
563 Arrows indicate wt (lower) and mutated (40 kDa higher) eIF2 $\alpha$  bands. Tubulin was used as a loading control. B,C.  
564 Cell death detected by flow cytometry in K562 wt, eIF2 $\alpha$ S51A and S51A shUTR mutant cells in untreated  
565 conditions (B) or after treatment with 0,5 and 1  $\mu$ M imatinib (C). Data are shown as a percentage of dead cells  
566 measured using AnnV/7AAD assay. Statistical analysis: Unpaired t test with Welch's correction (\*p  $\leq$  0.05; \*\*p  $\leq$   
567 0.005; \*\*\* p  $\leq$  0.0005).

568

569 **Figure 2. Pharmacological treatment with ISRB or GSK157 impairs the ISR activation in K562 leukemic**  
570 **cells *in vitro*.**

571 A. Schematic graph of the ISR signaling pathway with the site of ISRB and GSK157 action. B, C. CHOP and  
572 GADD34 mRNA expression levels measured by RT-qPCR in K562 cells. Cells were preconditioned with either  
573 ISRB or GSK157 inhibitors in indicated concentrations, followed by ISR induction by 100nM thapsigargin for 2  
574 hours. The level of not treated cells (CTR) was used as a reference =1. Statistical analysis: unpaired Student's t-  
575 test with Welch's correction and p  $\leq$  0,05 was estimated as significant (\*p  $\leq$  0.05; \*\*p  $\leq$  0.005; \*\*\*p  $\leq$  0.001; \*\*\*\*p  $\leq$   
576 0.0005).

577

578 **Figure 3. ISRB, but not GSK157, sensitizes K562 CML cells to imatinib *in vivo*.**

579 A. The workflow of the *in vivo* experiment. Mice were: not treated (n=12); or treated with: imatinib (n=14); imatinib  
580 and GSK157 (n=13); imatinib and ISRB (n=12). B. The number of mice which were injected with K562 cells and  
581 mice which developed tumors upon all tested conditions. C. The pictures of tumors isolated from representative  
582 experiment presenting the differences in proliferation potential of K562 cell in indicated variants. D. Corresponding  
583 graph showing the tumor mass. Tumors grown in mice injected with K562 cells and treated with imatinib were  
584 used as a control = 100%. Statistical analysis: Unpaired t-test, F-test to compare variances (\*p  $\leq$  0.05; \*\*p  $\leq$   
585 0.005).

586

587 **Figure 4. ISRib in combination with imatinib attenuates engraftment of primary TKI refractory CML CD34+  
588 blasts.**

589 A. The workflow of the *in vivo* experiment. PDX mice were: not treated/vehicle administrated (n=7); or treated  
590 with: imatinib (n=6); ISRib (n=7); or combination of imatinib and ISRib (n=7). B. Weight of spleens isolated from  
591 mice not treated or treated as indicated. C. Representative density plots showing the engraftment of hCD45+  
592 CML primary cells into the bone marrow population under therapeutic treatment, detected by flow cytometry.  
593 hCD45+ population is gated on the hCD45 vs SSC dot plots, the percentage of hCD45+ cells is indicated. D, E.  
594 Corresponding graphs showing the bone marrow (D) or spleen (E) engraftment estimated by flow cytometric  
595 detection of hCD45+ CML primary cells in bone marrow or spleen, respectively, in given variants of treatment.  
596 The percentage of hCD45+ cells is shown. Statistical analysis: Unpaired t test, F test to compare variances (\*p ≤  
597 0.05; \*\*p ≤ 0.005; \*\*\*p ≤ 0.0005).

598

599 **Figure 5. Combination of ISRib and imatinib results in reprogramming of gene expression profile of  
600 primary TKI-resistant blasts.**

601 A. Two-dimensional principal component analysis plot of samples based on gene expression (TPM) data obtained  
602 from FACS-sorted hCD45+ CML cells isolated from untreated control mice (n=2, blue), or treated with ISRib (n=3,  
603 red), imatinib alone (n=3, orange) or with combination of imatinib and ISRib (n=3, green). B. Hierarchically  
604 clustered heatmap of fold-changes in expression (log2FoldChange) of significantly differentially expressed genes  
605 between the indicated pairs of conditions. Pairwise correlations of expression fold-changes are also shown. C.  
606 Significantly altered genes upregulated (positive value on x-axis) or downregulated (negative value on x-axis) in  
607 combined imatinib and ISRib treatment versus with imatinib alone. D. Clusters (C0-C12) of co-expressed genes  
608 with varying patterns of gene expressions across all variants of treatment. Clusters C0, C1 displaying sharp  
609 downregulation or C5, C6 showing sharp upregulation of gene expression after combined treatment are marked in  
610 blue frame. E. Diagram showing the percentage of genes identified in four selected clusters C0, C1, C5, C6 (blue)  
611 and the rest (grey).

612

613 **Figure 6. Co-expressed genes downregulated upon combined treatment are related to RAS/RAF/BRAF  
614 and Interferon gamma signaling.**

615 Functional enrichment Reactome (REAC<sup>66</sup>) terms significantly enriched in C0, C1, C5 and C6 clusters.  
616 Downregulated genes belonging to C0, C1 clusters are indicated. RAS signaling is marked in red color, Interferon  
617 gamma signaling is marked in blue color.

618

619

620

621 **Figure 7. Combination of imatinib and ISRIB attenuates STAT5 signaling in CML cells.**

622 A, B. Left panels: Protein levels of STAT5 and phosphorylated form of STAT5 (pSTAT5) detected by western blot  
623 in K562 (A) or LAMA84 (B) CML cells untreated (control) or treated with drugs as indicated (all variants  
624 tapisargin treated). The ratio of phosphorylated to total STAT5 forms (P/T) calculated based on the densitometry  
625 signal is given for each condition. A, B. Right panels: Adequate graphs showing pSTAT5/STAT5 ratios in K562  
626 cells (A) and LAMA84 CML cells (B). Signal for control cells (without drug treatment) =1. Statistical analysis:  
627 unpaired T-test with Welch's correction (\*p ≤ 0.05; \*\*p ≤ 0.005; \*\*\*p ≤ 0.0005). C. Flow cytometry analysis of  
628 pSTAT5 levels in K562 (left panel) and LAMA84 (right panel) cells untreated (control) or treated as indicated.  
629 Data were calculated based on gMFI, fluorescence signal for untreated cells=1. Statistical analysis: repeated-  
630 measures one-way ANOVA, with Tukey's multiple comparisons test (\*p ≤ 0.05). D. Overlay of the representative  
631 histograms presenting fluorescence signals for pSTAT5 estimated in control cells or in cells after treatment. gMFI  
632 values are indicated for each condition. E. The heat map showing expression level (transcript per kilobase million  
633 or TPM, standardized with z-score) of STAT5-target genes belonging to C0, C1 clusters shown for each gene  
634 across all replicates of untreated (control) and treatment conditions. F. The change in expression of STAT5-target  
635 genes belonging to cluster C0 and C1 in treatments comparison: expression fold change (log2FoldChange) in all  
636 comparisons.

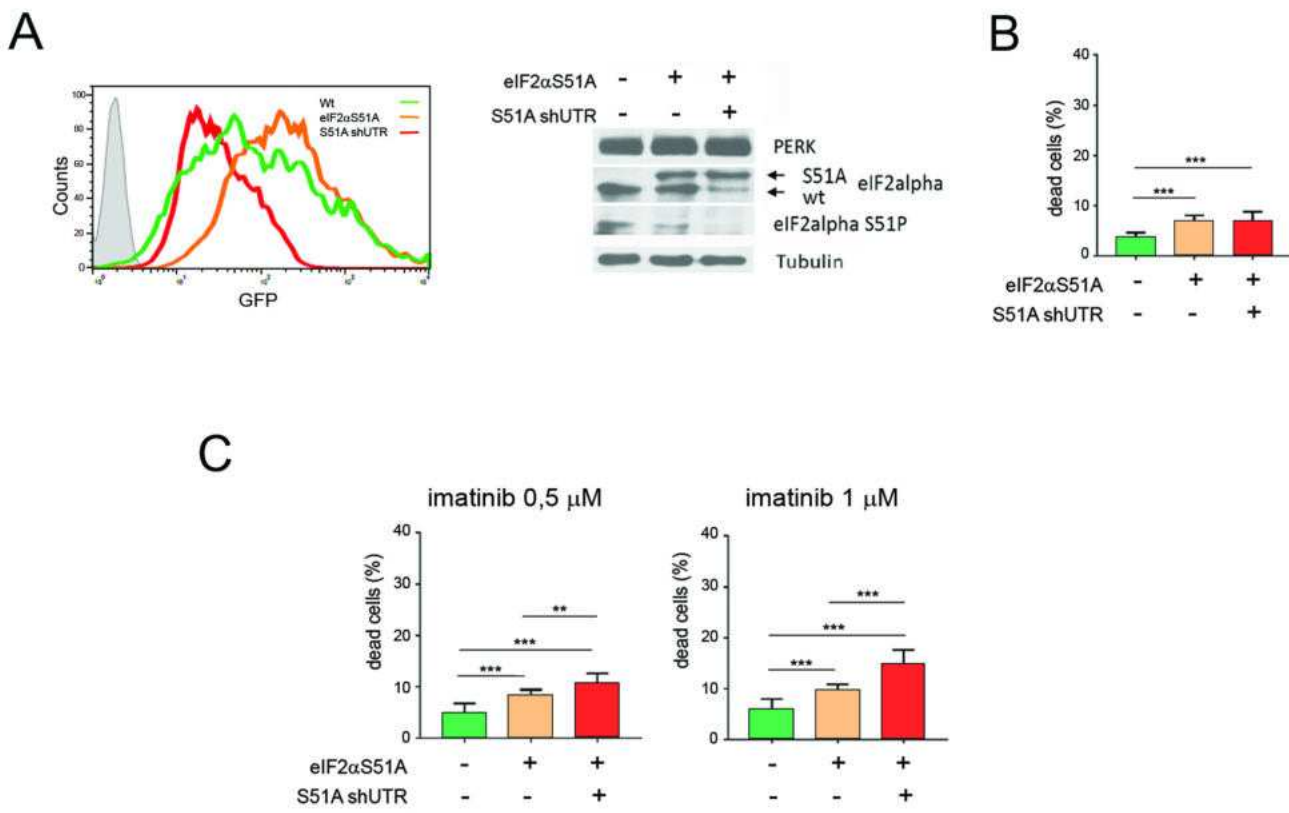
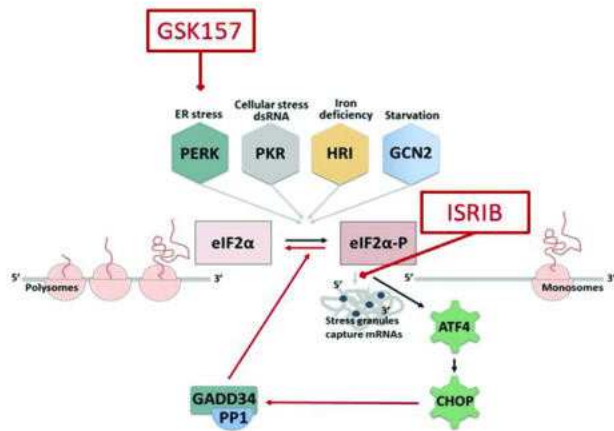
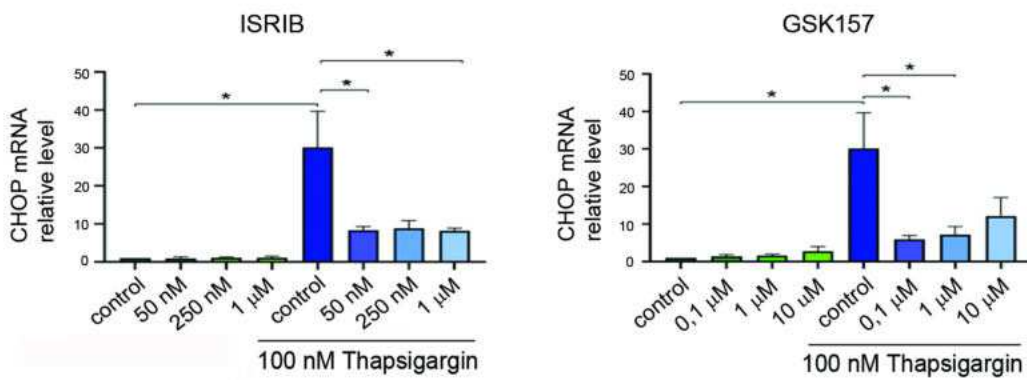
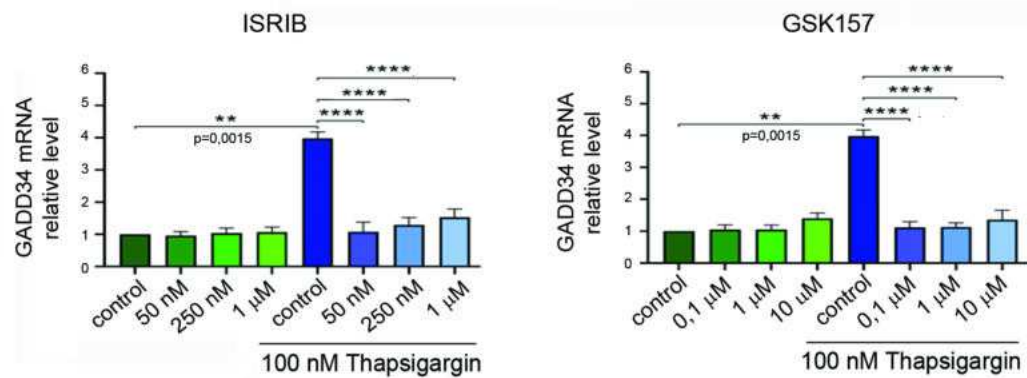
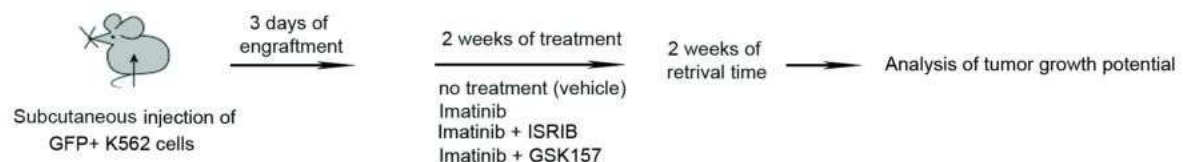
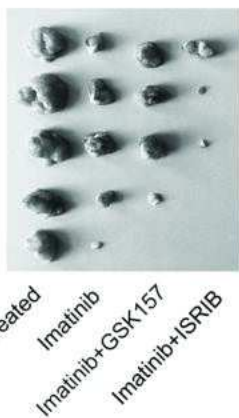
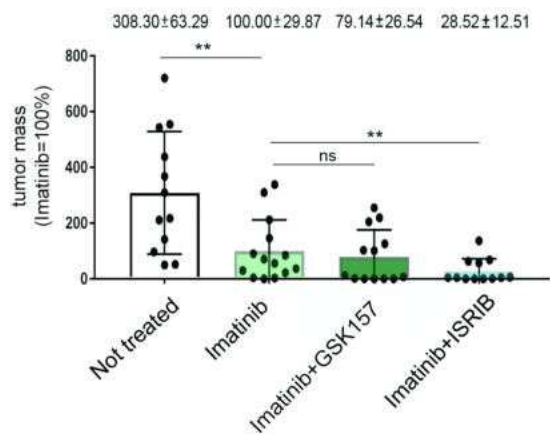


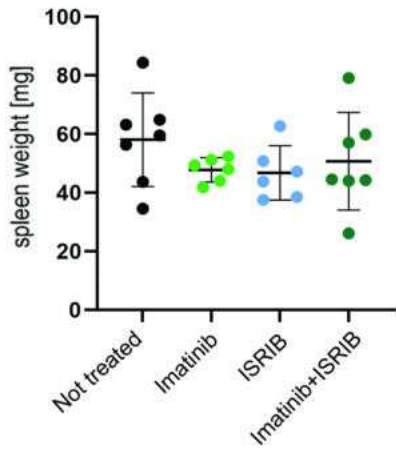
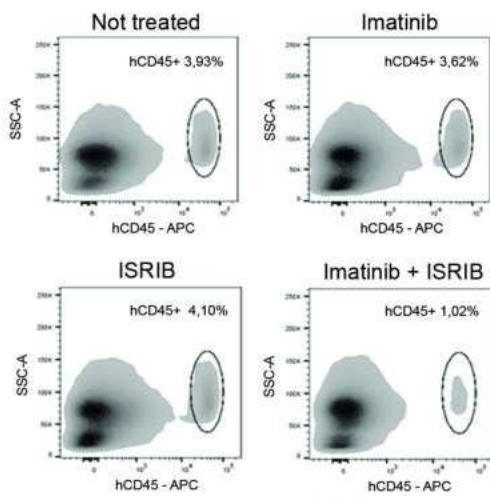
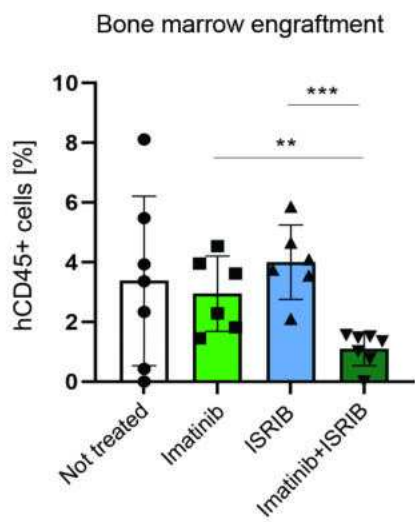
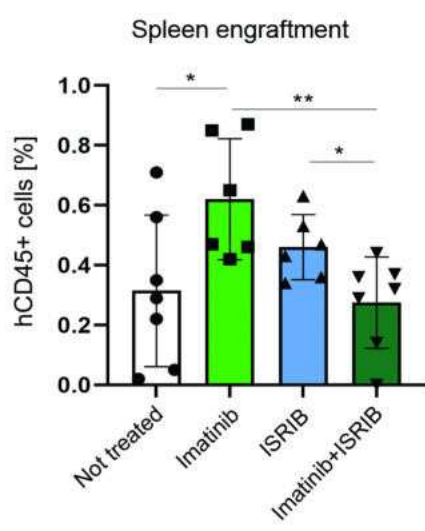
Figure 1

**A****B****C****Figure 2**

**A****B****Tumor formation**

	Number of mice injected with CML cells	Number of mice with detected tumors
Not treated	12	12
Imatinib	14	12
Imatinib + GSK157	13	9
Imatinib + ISRIB	12	5

**C****D****Figure 3**

**A****B****C****D****E****Figure 4**

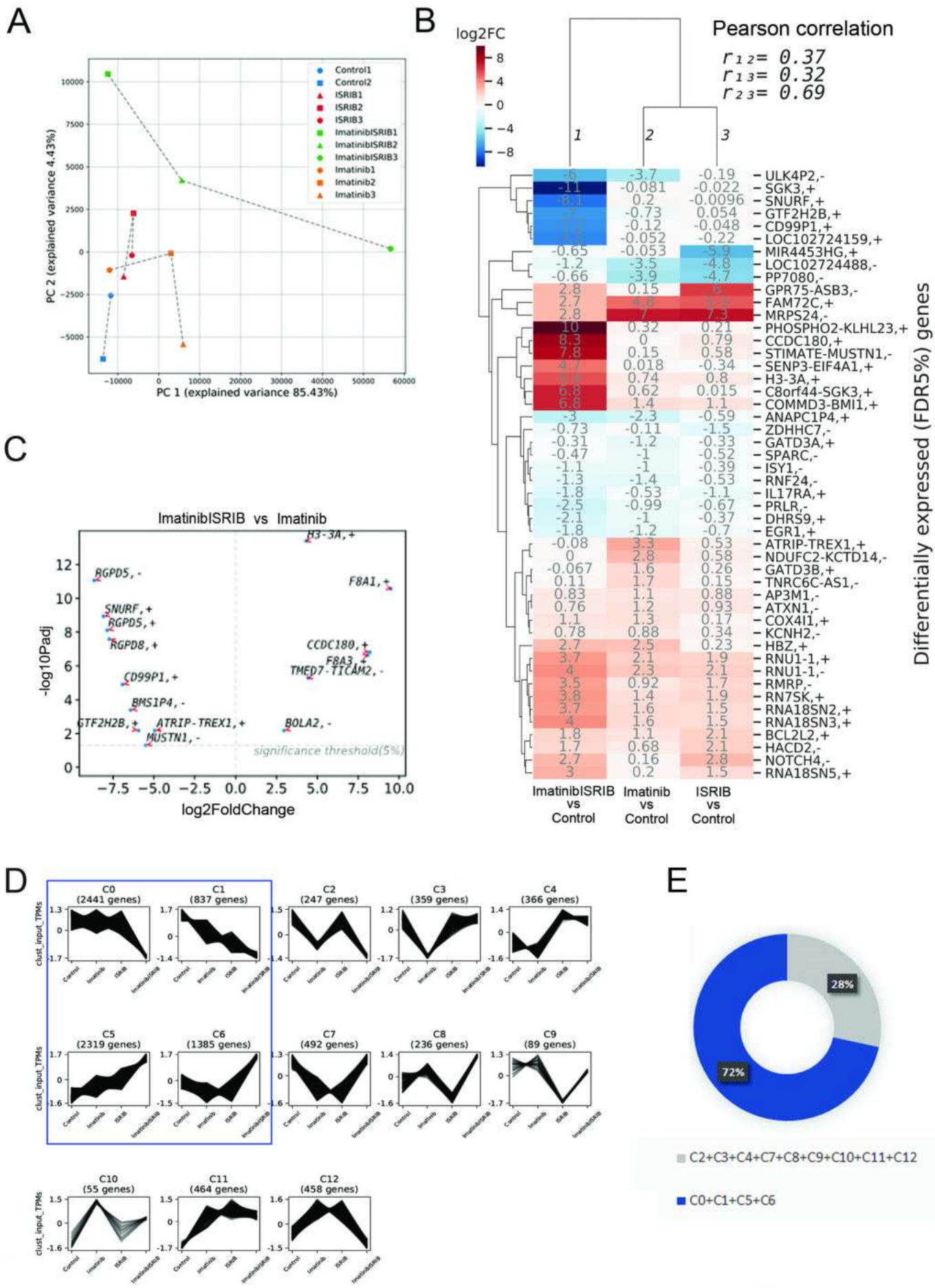


Figure 5

## enriched REAC terms

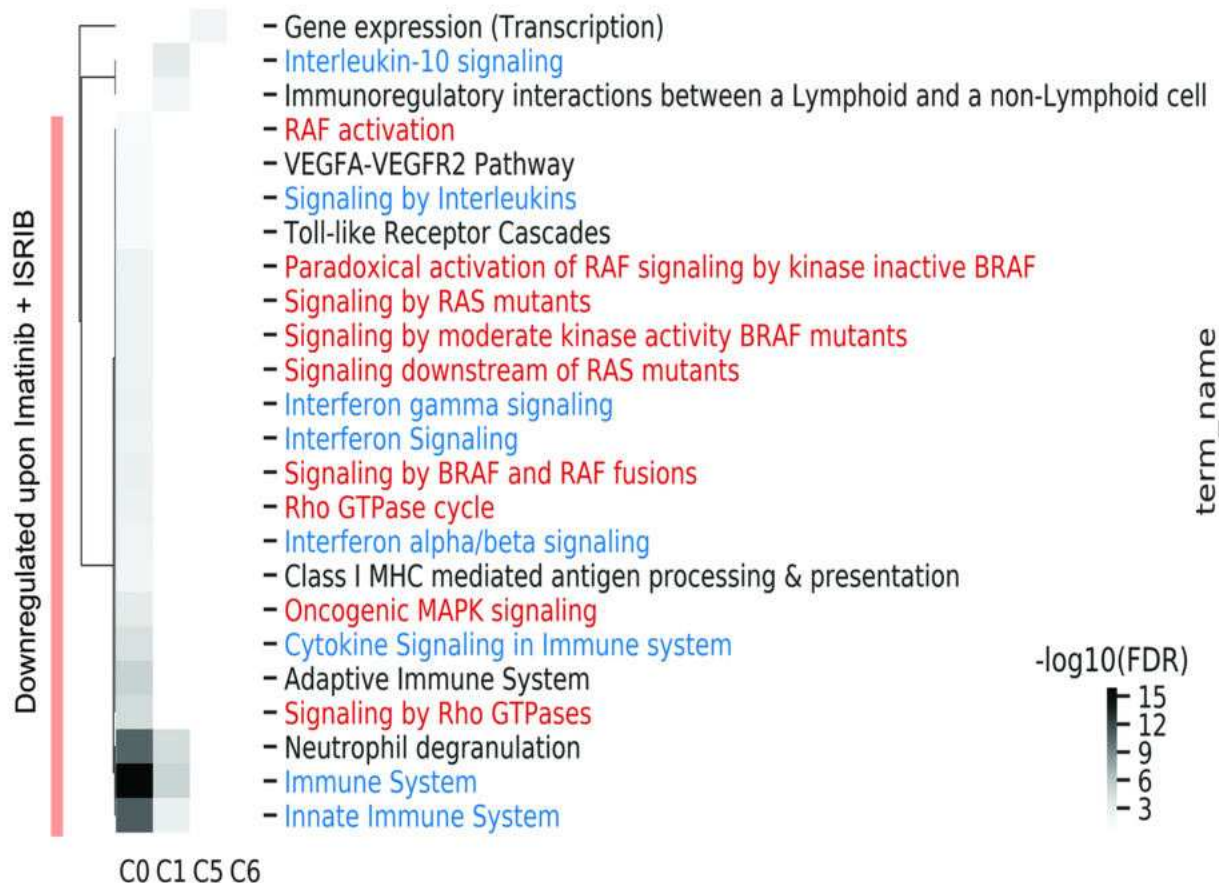


Figure 6

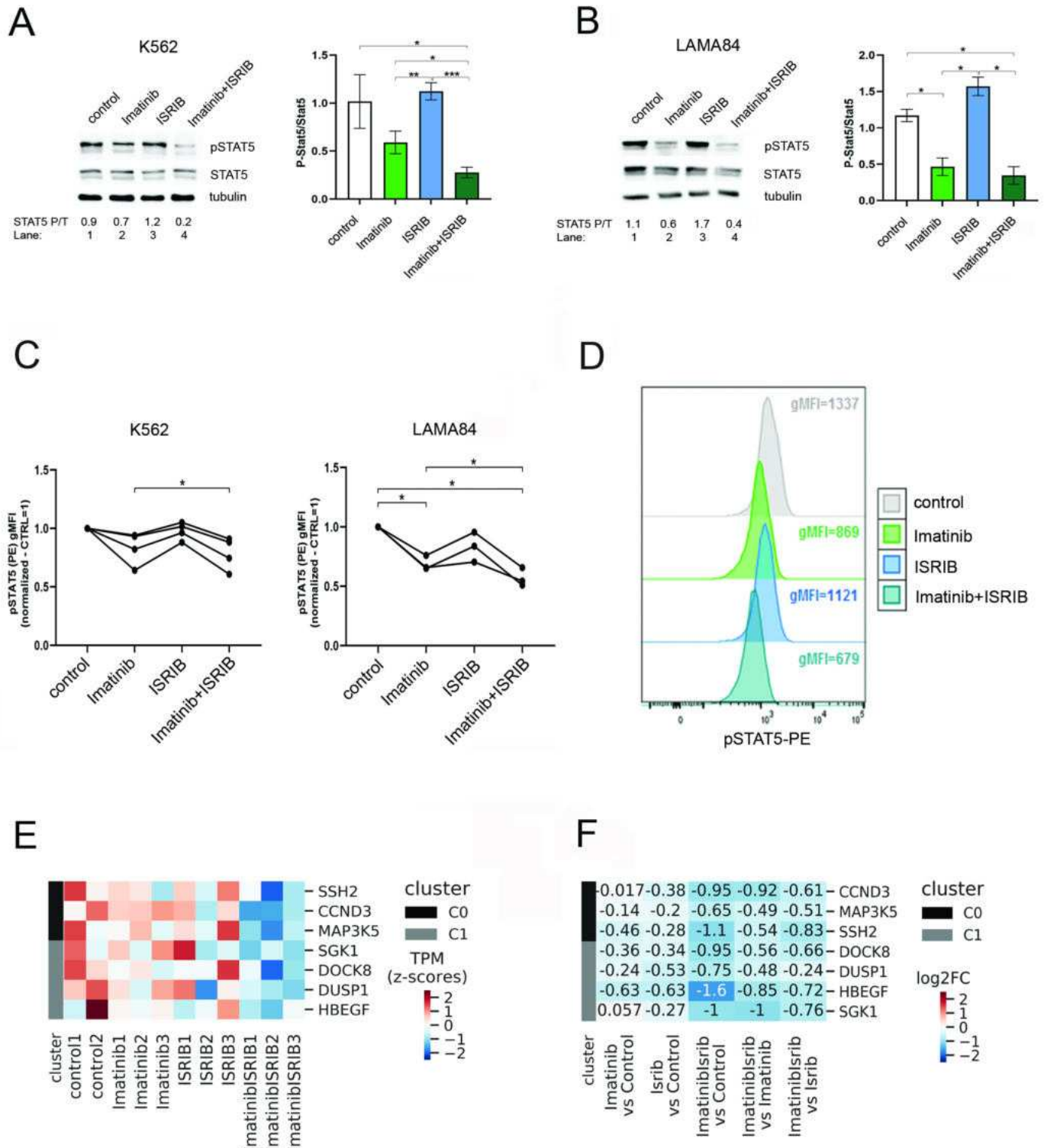


Figure 7